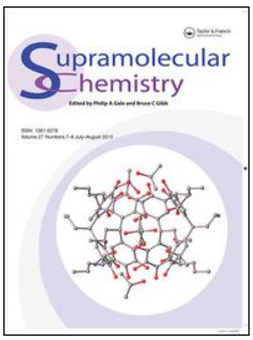

Supramolecular Chemistry

ISSN: 1061-0278 (Print) 1029-0478 (Online) Journal homepage: https://www.tandfonline.com/loi/gsch20

A highly selective ratiometric fluorescent probe for H_2S based on new heterocyclic ring formation and detection in live cells

Sandip Kumar Samanta, Syed Samim Ali, Ankita Gangopadhyay, Kalipada Maiti, Ajoy Kumar Pramanik, Uday Narayan Guria, Aritri Ghosh, Pallab Datta & Ajit Kumar Mahapatra

To cite this article: Sandip Kumar Samanta, Syed Samim Ali, Ankita Gangopadhyay, Kalipada Maiti, Ajoy Kumar Pramanik, Uday Narayan Guria, Aritri Ghosh, Pallab Datta & Ajit Kumar Mahapatra (2019): A highly selective ratiometric fluorescent probe for H_2S based on new heterocyclic ring formation and detection in live cells, Supramolecular Chemistry, DOI: 10.1080/10610278.2019.1590573

To link to this article: https://doi.org/10.1080/10610278.2019.1590573

SUPRAMOLECULAR CHEMISTRY
https://doi.org/10.1080/10610278.2019.1590573

Taylor & Francis
Taylor & Francis Group

ARTICLE

A highly selective ratiometric fluorescent probe for H_2S based on new heterocyclic ring formation and detection in live cells

Sandip Kumar Samanta[a], Syed Samim Ali[a], Ankita Gangopadhyay[a], Kalipada Maiti[a], Ajoy Kumar Pramanik[a], Uday Narayan Guria[a], Aritri Ghosh[b], Pallab Datta[b] and Ajit Kumar Mahapatra[a]

[a]Department of Chemistry, Indian Institute of Engineering Science and Technology, Shibpur,Howrah, India; [b]Centre for Healthcare Science and Technology, Indian Institute of Engineering Science and Technology, Shibpur, India

ABSTRACT

A 3-indolylacrylate derivative, **3-IA**, prepared by connecting an ethyl acrylate in 3-position of indole has been synthesised and characterised. Ethyl acrylate moiety acts as the Michael acceptor towards H_2S, and the resultant addition product then participates in intramolecular cyclisation with the ester group at 2-position to form another new heterocyclic ring. Blue fluorescence of **3-IA** turned into green in presence of H_2S, leading to ratiometric behaviour of the fluorescent sensor with large stokes shift of 55 nm. Probe **3-IA** has excellent selectivity towards H_2S over other biothiols and other competing anions. Density function theory/time-dependent density function theory calculations were carried out to validate the reaction mechanism and the electronic properties of **3-IA**. Importantly, the ratiometric probe **3-IA** shows great promise in H_2S detection by simple visual fluorescent inspection in filter paper-based protocol. The probe shows its excellent ability to detect H_2S in different natural water samples. Furthermore, we have employed our probe to detect H_2S for ratiometric imaging in live Vero cell.

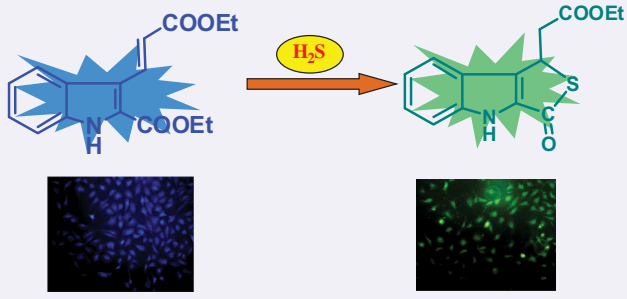

ARTICLE HISTORY
Received 28 August 2018
Accepted 25 February 2019

KEYWORDS
Ratiometric sensor; hydrogen sulfide; DFT/TDDFT calculations; detection in various water sample; cell imaging

1. Introduction

A reaction-based chemosensor, named as chemodosimeter, has a proficient application due to irreversible chemical reaction with the external stimuli. Upon interaction with those external stimuli, receptors unit change their electronic properties which are the basis of the molecular recognition. Although lots of derivatives of indole and thiophene have been prepared, an indole-conjugated thiophene compound is still in investigation. For the best of our knowledge, till, not much devotion has been employed around this field of chemistry. Thus, our aim of this work mainly focused on designing an organic protocol which upon treatment with an analyte will produce those indole–thiophene-coupled derivatives. Thus, in this work, we have prepared a new heterocyclic compound via hydrogen sulfide detection technique.

Hydrogen sulfide (H_2S), the simplest biothiol, has been considered as the gaseous molecular messenger in a variety of human biological systems (1–4). Like other reactive small molecules (5–7) eg. carbon monoxide (CO) and nitric oxide (NO), endogenous H_2S is used by various organisms extending from bacteria to mammals for production of energy, signal transduction, and response in immune system (8–10). 3-Mercaptopyruvate sulfur transferase, cystathionine-γ-lyase (CSE), and cystathionine β-synthase (CBS) are such enzymes, responsible for the formation of endogenous H_2S in a certain catalytic reaction (11, 12).

CONTACT Ajit Kumar Mahapatra mahapatra574@gmail.com Department of Chemistry, Indian Institute of Engineering Science and Technology, Shibpur, Howrah 711103, India

Supplemental data for this article can be accessed here

Toxicity and hence lethal effect of H_2S are attributed as it is a colourless, highly water-soluble, and flammable gas with an unpleasant rotten egg smell (13). So, the irregular levels of H_2S are strictly related to many diseases, for example, slow growth, Alzheimer's disease, cardiovascular disease, Down's syndrome, diabetes, osteoporosis, leucocyte loss, cancer, and liver cirrhosis (14–20).

Therefore, to better comprehend the role of H_2S in pathological and physiological processes, the recognition of H_2S has become a vital topic of scientific research, especially in biological systems (21). A number of analytical techniques have been reported for the detection of H_2S, like gas chromatography and electrochemical (22) and colorimetric (23) methods. But, due to the short lifetime of H_2S in live cells, these approaches experience complications in preserving precision and real-time imaging.

Recently, fluorescent chemodosimeters have fascinated a considerable devotion due to the benefit of high sensitivity, selectivity, and real-time detection (24–26). To date, lots of fluorescent sensors for H_2S have been reported so far. Mostly, reduction of azide and nitro functionality, nucleophilic addition, and coppersulfide precipitation-based fluorescent probes have been reported for H_2S detection (27–41). These sensors are highly efficient at the task they are designed to perform. However, there is still room for new ideas in this field. Cleavage of dinitrophenyl ether group has become an interesting approach for H_2S detection. Some design strategies relied on intramolecular cyclisation followed by regeneration fluorescent moiety. In a few cases, S^{2-} were recognised in terms of secondary analyte detection from a metal-bound ensemble. Recently, dinitrophenyl ether group incorporated into a lysosome-targeted 1,8-naphthalimide fluorophore for live cell imaging of H_2S has been reported by Tang *et al*. (42). A mitochondria-targeted fluorescent sensor for detection of H_2S has been explored by Yoon et al., where the response time is 40 min (43). Merocyanine-based fluorescent chemodosimeters for the detection of H_2S over other interfering biothiols have been synthesised by three independent groups of authors, namely, Guo, Zhao and Goswami *et al*. (44–46). In their strategy, an electrophilic indolium part of merocyanine unit is responsible for the facile nucleophilic reaction of S^{2-}/SH^{-} which is accompanied by a change in optical properties. Recently our group reported a merocyanine-based dual-reactive centre for H_2S, wherein the low the H_2S concentration, the more reactive indolium moiety was reacted and then the dinitrophenyl-ether part was cleaved upon increasing the analyte concentration (47). As manifested by Holmes *et al*. that at a physiological pH, simple thiols can react readily with some Michael acceptors. But, due to fast equilibrium, the products could not be obtained or recognised from the reaction mixture (48). Anchored in Holmes' fallout, we proposed that, due to the high reactivity of H_2S over the biothiols, certain Michael acceptors might be helpful to distinguish H_2S from biological thiols by stimulating the intramolecular cyclisation reaction at physiological pH. For instance, biothiols have a nucleophilic sulfhydryl group (–SH) and the pKa of H_2S (6.9) is lower than that of Hcy (8.9), Cys (8.3), or GSH (9.2), demonstrating that H_2S has a higher nucleophilicity than other biothiols under physiological conditions. Therefore, it is effortless to discriminate Hcy/Cys/GSH from H_2S simply via nucleophilic reaction-based strategies in physiological media. In this respect, Xian group has successfully developed this type of fluorescent chemosensors for the selective detection and bioimaging of H_2S (49). Nevertheless, in Table S7, (50-57) we have compared some recent H_2S probes with our probe in different aspects.

Detection of H_2S through the formation of S-heterocycle, coupled with indole in a ratiometric manner.

Herein, we have designed a 3-indolylacrylate derivative, **3-IA**, by connecting an ethyl acrylate in 3-position of indole as Michael acceptor and an ester group ortho to ethyl acrylate was employed as a specific function for cyclisation via intramolecular nucleophilic attack. In particular, ratiometric fluorescent probes are always favoured to 'on-off' or 'off-on' response as they are able to evade fake detection and improved signal-to-noise ratio as the detection occurs by using the intensity ratio of two different wavelengths. The philosophy of the design lies in that the methylene malonate will trap H_2S through Michael reaction to yield an intermediate **3-IASH** moiety, which can undergo tandem intramolecular nucleophilic attack on the reactive ester carbonyl group, present in suitable position, through a five-membered cyclic transition state, illuminating blue to green emission. Thus, the design strategy revealed a route for the synthesis of the indole–thiophene-coupled new heterocyclic compound. In adddition to this no ratiometric fluorescent response was observed when probe 3-IA reacts with other biothiols. Based on the above reaction strategy, highly discriminative detection of H_2S over other biothiols can be successively employed. However, the detection limit is not as impressive as that of some other reported H_2S probe (58). The sensing mechanism involving nucleophilic attack at electrophilic centre leading to cyclisation that ultimately leads to ratiometric fluorescent spectral changes is an important aspect of this work. Most importantly, our design strategy is completely different from those

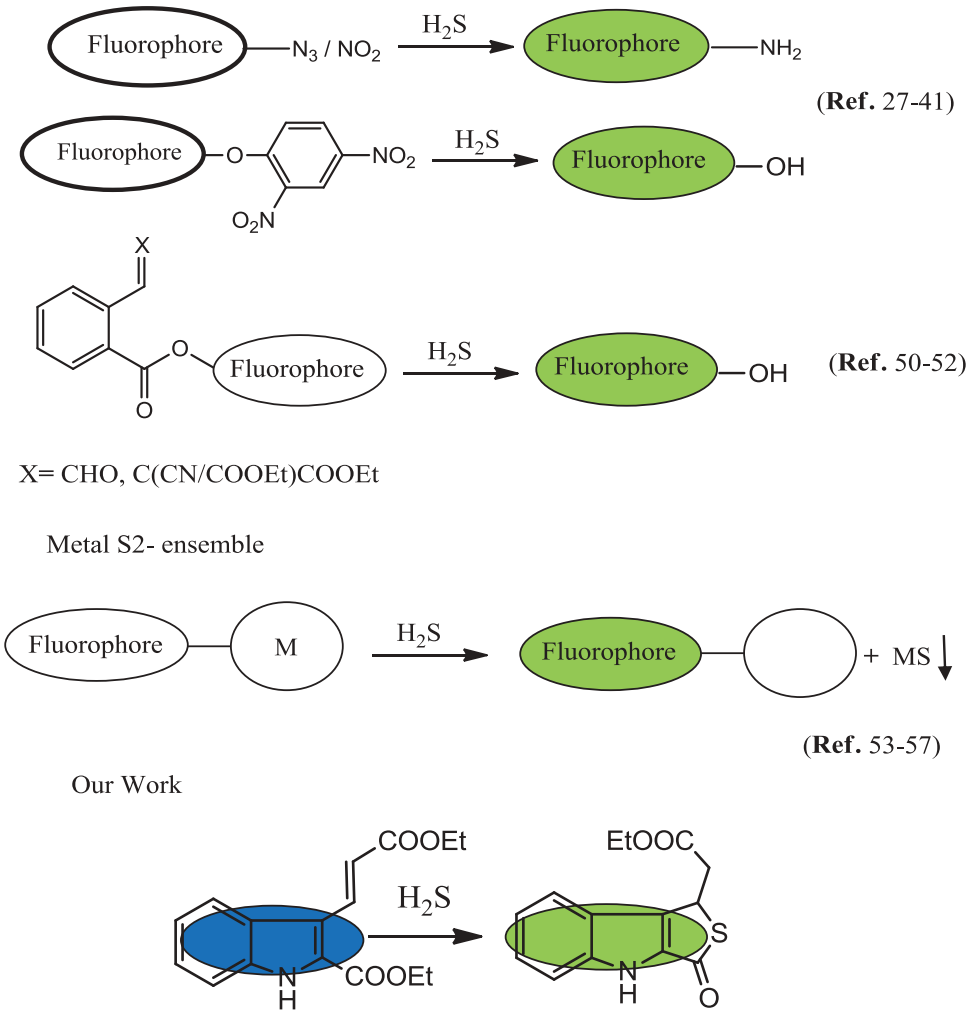

Scheme 1. Conventional way for detection of H_2S

previously reported techniques, especially in cases where nucleophilic addition of H_2S followed by regeneration of fluorescent moiety was occurred. Li *et al*. (59) reported a BODYPI-based sensor containing a conjugated ester unit placed in a close vicinity of an aldehyde group which acts as nucleophilic acceptor and in presence of H_2S undergo intermolecular cyclisation to form a new heterocyclic compound which was responsible for turn-on fluorescence response. But the response time and limit of detection towards H_2S was very high. Here, in our case, we have changed the design scheme by keeping an ester group to the close vicinity of the conjugated ester unit. Thus, we observed that the reaction rate is increased and the limit of detection of the probe to H_2S is reduced. Not only this, we have achieved a ratiometric fluorescence response upon treatment with H_2S which is, in turn, favourable than a turn-on sensor. Also, by using this design plan, we have able to synthesise a new heterocyclic compound, i.e. an indole-conjugated thiophene which is still an undiscovered compound to the chemist.

2. Results and discussion

2.1. Synthesis and characterisation

Probe **3-IA** can be readily synthesised in three steps starting from indole-2-carboxylic acid followed by the preparation of its ester and the subsequent formylation reaction according to the standard procedure outlined in Scheme 2. The probe molecule **3-IA** has been synthesised by the condensation of 2 with diethyl malonate in presence of piperidine. The structure of **3-IA** was recognised by ^{1}H-NMR spectroscopy, ^{13}C-NMR spectroscopy, LC-MS, and single crystal x-ray analysis (Supporting Information). Details of experimental procedure and data of characterisation of different structures are given in the Supporting Information.

2.2 UV-Vis study

Probe **3-IA** [10.0 μM in DMSO–H_2O (1:9), HEPES buffer; pH 7.4, 10 mM] itself showed two main

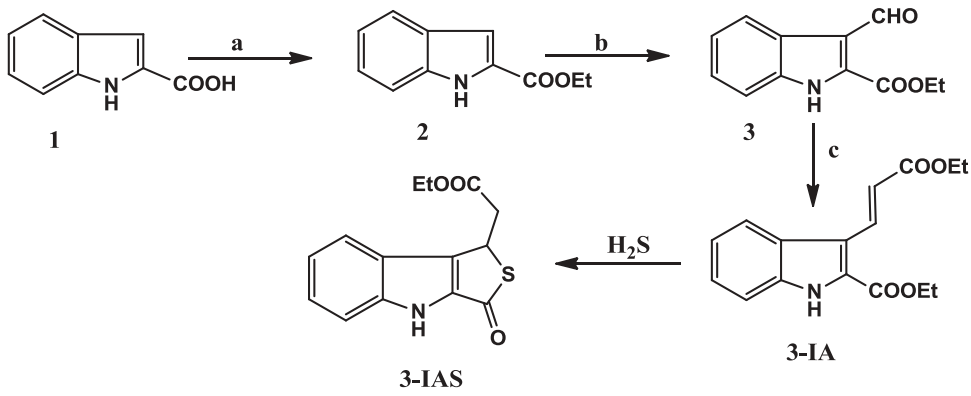

Scheme 2. Reagent and condition: (**a**) EtOH, H^+, reflux, 12 h, 70%; (**b**) DMF, $POCl_3$, 60°C, 35%; and (**c**) DEM, EtOH, piperidine, reflux, 24 h, 48%.

absorption bands at 278 and 354 nm. Then, to a fixed concentration (10.0 μM) of **3-IA**, varying concentrations of H_2S (using Na_2S as the equivalent source of H_2S) were added to evaluate the absorption titration. Addition of H_2S (0–12 equiv.) persuades a red shift in both the absorption peaks (Figure 1), resulting in two new absorption bands centred at around 309 and 414 nm, respectively, accompanied with the colour of the solution of **3-IA** changing from colourless to yellow (Figure 1(a)).

So, compound **3-IA** can serve as a 'naked-eye' sensor for H_2S. Three distinct isosbestic points at 290, 320, and 378 nm indicate the formation of a new compound upon reaction of probe **3-IA** with H_2S.

2.3 Fluorescence study

Upon excitation at 308 nm, sensor **3-IA** [10.0 μM in DMSO–H_2O (1:9), HEPES buffer; pH 7.4, 10 mM] displayed an intense emission band at 408 nm.

However, as revealed in Figure 2(a), the addition of H_2S evoked a drastic decrease in the emission intensity at 408 nm, and the concurrent appearance of a new emission band at 463 nm accredited to the thiol-mediated cyclisation. The free probe exhibited a blue emission colour, and the addition of H_2S elicited a significant variation in emission colour from blue to green. Thus, the probe provided a substantial ratiometric fluorescent response (I_{463}/I_{408}) from 0.3259 to 5.0746 (a 15.57-fold enhancement) upon addition of 12 equiv. of H_2S (Figure 2). Figure 2(b) shows a graph of the ratio of fluorescence intensity (F_{463}/F_{408}) of the

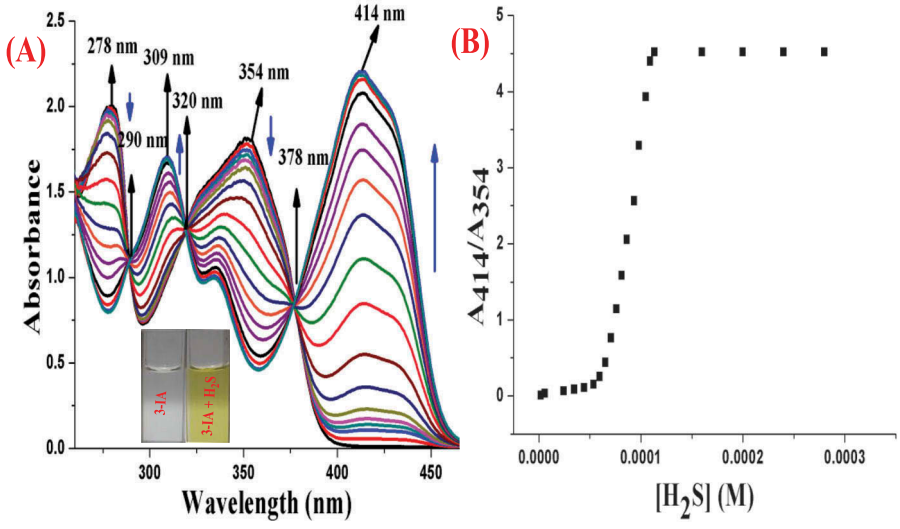

Figure 1. (colour online) (a) Absorption spectra of **3-IA** (10.0 μM) upon addition of H_2S (0–12 equiv.) (HEPES buffer, pH = 7.4). (b) Absorbance intensity ratio changes (A_{414}/A_{354}) of **3-IA** (10.0 μM) upon addition of various concentrations of H_2S.

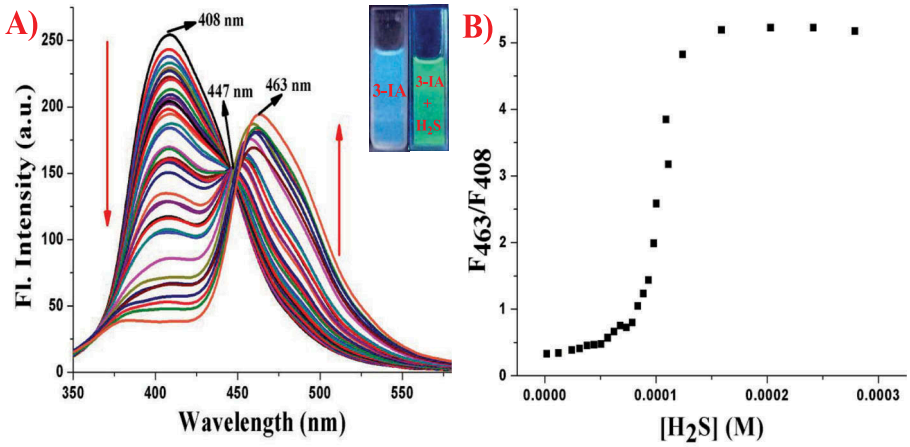

Figure 2. (colour online) (a) Emission spectra of **3-IA** (10.0 μM, λ_{ex} = 308 nm) upon addition of H_2S (0–12 equiv.). (b) Fluorescence intensity ratio changes (F_{463}/F_{408}) of **3-IA** (10.0 μM) upon concomitant addition of H_2S (0–12 equiv.).

sensor **3-IA** against the concentration of H_2S starting from 0 to 50.0 μM. From the above-mentioned graph, the corresponding linear fit (R^2 = 0.998) has been drawn to the experimental data. From the linear fit of the experimental data, the limit of detection **3-IA** for H_2S was calculated to be 1.7 μM. (Figure S9 of the Supplementary Information, available online).

2.4 Interference studies

Further, to test the efficient applications of sensor **3-IA** as a ratiometric fluorescent probe for H_2S, the fluorescence response of probe **3-IA** to H_2S in the presence of typical competing species such as various anions F^-, Cl^-, Br^-, I^-, SO_4^{2-}, HSO_3^-, and $S_2O_3^{2-}$ and related thiol-containing compounds (Cys, Hcy, and GHS) was studied (Figure 3).

As shown in Figure 3(b), during titration of allied ions with the probe, no significant fluorescence increase was observed. To examine whether probe **3-IA** could still hold on to the sensing response to H_2S in the incidence of different potential competitive analytes, the probe **3-IA** (10.0 μM) was treated with H_2S in the presence of F^-, Cl^-, Br^-, I^-, SO_4^{2-}, HSO_3^-, and $S_2O_3^{2-}$ (Displayed in Figure S10 of the Supplementary Information, available online). All the pertinent analytes examined have almost no impact on the fluorescent detection of H_2S. Furthermore, when biothiols (1 mM) and H_2S (10 μM) have coexisted, we are able to notice ratiometric fluorescence change using this probe. These results established that the ratiometric response of probe **3-IA** was highly selective for H_2S and could be served for the detection and discrimination of H_2S in presence of a high concentration of interfering biothiols. Notably, no visible variations were observed upon addition of other biological thiols, but the huge ratiometric fluorescent response delivered the probe suitable for detection of H_2S by easy visual assessment and

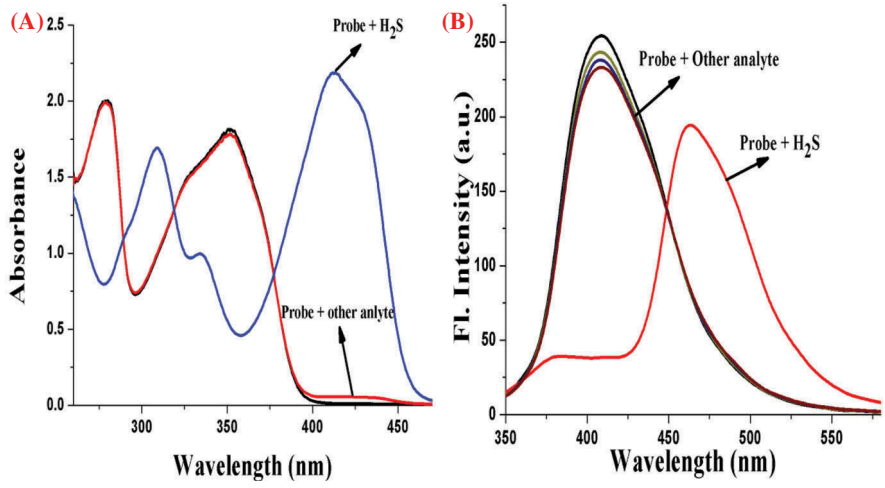

Figure 3. (colour online) (a) Absorption spectra of **3-IA** (10.0 μM) in presence of various analytes (50.0 μM) in aqueous DMSO (DMSO:H_2O = 1:9 v/v, 10.0 mM HEPES buffer, pH = 7.4). (b) Fluorescence spectra of probe **3-IA** (10.0 μM) in presence of various analytes (50.0 μM) in aqueous DMSO (DMSO:H_2O = 1:9 v/v, 10 mM HEPES buffer, pH = 7.4).

established the potential ability of the sensor **3-IA** for detection of H_2S in biological systems.

2.5 Kinetic study

Next, we wish to look at the kinetic profiles of the reaction in the fluorescence method (at 463 nm) in different concentrations of Na_2S at room temperature. Initially, the pseudo-first-order rate constant (K_{obs}) was calculated by using the following equation: $\ln (F_{max} - F_t)/F_{max} = - K_{obs} \times t$. For this purpose, the time-dependent fluorescence experiments were also carried out on probe **3-IA** (10.0 μM) with various concentrations of Na_2S (5, 10, 15, and 20 equiv.). As observed from Figure 4, the fluorescence intensity at 408 nm decreases, while fluorescence intensity at 463 nm increases with reaction time.

The higher concentration of Na_2S resulted in a faster reaction and pronounced fluorescence enhancement. The ratio of fluorescence intensities (F_{463}/F_{408}) increases with reaction time and gets saturated within 15 min. So, the H_2S-mediated cyclisation reaction was found to follow a pseudo-first-order rate law of rate constant $k' = 0.292$ min^{-1} (Figure S12 of the Supplementary Information, available online) under excess H_2S concentration. In addition, the second-order rate constant was also evaluated by calculating the linear fit between k_{obs} and the H_2S concentration, and it was to be 192.67 $M^{-1}Min^{-1}$ (Figure S13 of the Supplementary Information, available online).

2.6. pH study

To be useful in the practical applicability, we also studied the emission behaviour of **3-IA** treated with H_2S in different pH environments. The probe, in the absence of H_2S, is stable over a broad range of pH values from 4 to 11 and works well between pH 5.0 to 8.0 in response to H_2S (Figure 5).

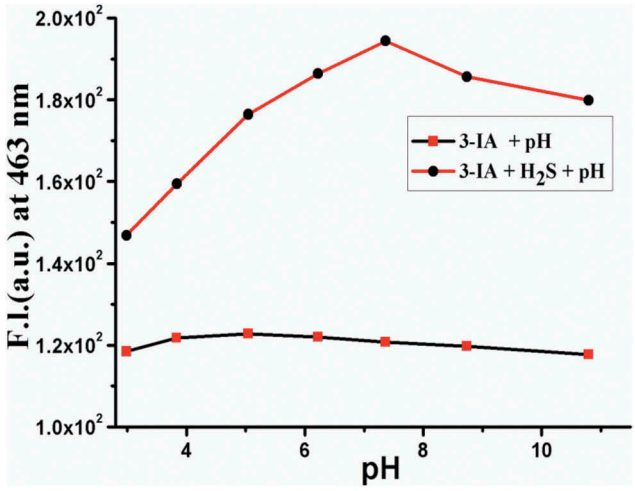

Figure 5. (colour online) pH-dependent fluorescent spectra of **3-IA** in the absence (black line) and in the presence (red line) of H_2S.

However, with the addition of H_2S, the fluorescence intensity at 463 nm augmented appreciably in the pH range of 6.5–7.8, which implies that the probe may work well under these physiological conditions. When the pH beat the value 8.0, the emission intensity drops down because of poor reactivity of H_2S at high pH, and at lower pH, emission intensity sharply decreased because of protonation of H_2S. The results indicate that **3-IA** works well in physiological pH circumstances.

2.7 Study of the reaction mechanism

Based on the observations on UV and fluorescent behaviour of the probe in presence of H_2S, we suggest the

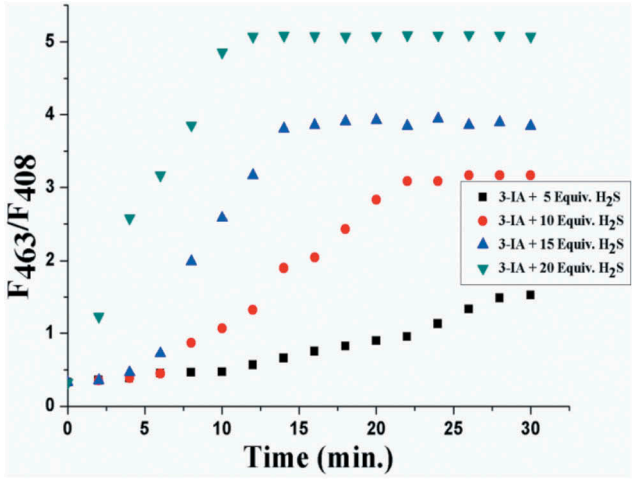

Figure 4. (colour online) F_{463}/F_{408}vs time plot **3-IA** (10.0 μM) in DMSO–H_2O (1:9, v/v) solution upon addition of different concentrations of H_2S λ_{ex} = 308 nm; λ_{em} = 463 nm.

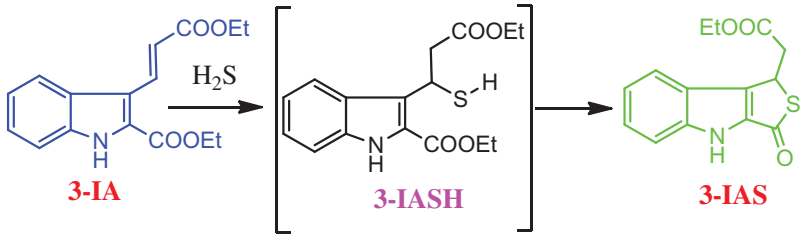

Figure 6. (colour online) Proposed sensing mechanism.

probable mechanism as shown in Figure 6. The product of this process was extracted from the reaction mixture and characterised in order to achieve evidence to support this mechanistic proposal.

^{1}H-NMR analysis of the product revealed that it contains the structure constituted by the ring formation through Michael addition of H_2S, and subsequently an intramolecular cyclisation yielded compound **3-IAS**. The resonance signal analogous to the alkene protons at 8.62 and 6.11 ppm moved out along with the aspect of two new peaks at 4.32 and 3.29 ppm designated to the methane and methylene protons of the compound **3-IAS**. LCMS spectrum analysis also confirmed the cyclisation reaction between H_2S and **3-IA**. For probe **3-IA**, a characteristic peak at m/z = 287.1 was obtained which is responsible for **[3-IA]**$^+$. Upon addition of H_2S, a new peak at m/z = 275.1 (assigned to the cyclise product) appeared, whereas peak at m/z = 287.1 was disappeared (Figures S4 andS8 of the Supplementary Information, available online).

2.8 Theoretical study

The electronic behaviour of the compound **3-IA** and its corresponding cyclic product **3-IAS** upon reaction with H_2S was explored using density function theory (DFT) and time-dependent density function theory (TDDFT) calculation at the B3LYP/6-31G(d) level of the Gaussian 09 program. The most effective geometries and calculated electron distributions in the frontier molecular orbital's HOMO and LUMO of the probe **3-IA** and its cyclic product **3-IAS** are shown in Figure 7(a). Main chromophoric unit indole moiety exists in a nearly planar conformation with ethyl acrylate part. These planar structures permit a proficient π-conjugation and esteem the Internal Charged Transfer (ICT) transition between the donor indole -NH and the acceptor acrylate group. In particular, the HOMOs and LUMOs of the probe **3-IA** and its cyclic product are widely spread out over the indolyl part. Additionally, the energy difference between the HOMO and LUMO of the probe **3-IA** was larger, 100.25 kcal/mol, than that of its corresponding cyclic product **3-IAS**, 64.67 kcal/mol (Table S2 in Supplementary Information), responsible for the bathochromic shift in the absorption spectra observed upon the treatment of probe with H_2S. Furthermore, TDDFT calculations clarify the electronic properties of the probe **3-IA** and its corresponding cyclic product **3-IAS**. The vertical main transitions, i.e. the calculated λ_{max} and oscillator strength (*f*), are scheduled in Table S1 in Supplementary Information, available online.

The vertical transitions calculated by TDDFT of **3-IA** and its cyclic product show good concurrence with the experimental data. The experiment recommends that the vertical transitions observed at ~359 and ~319 nm are analogous to those of the practically observed spectra at ~354 and ~309 nm for **3-IA** and its cyclic product, **3-IAS**, respectively. The main fundamental transitions for **3-IA** and its cyclic product, **3-IAS**, are $S_0 \rightarrow S_1$ (~69.10%) and $S_0 \rightarrow S_2$ (~68.50%), respectively, which corresponds to energy states arises from HOMO→LUMO and HOMO-1→LUMO, respectively. Thus, the calculated red shift is accord with experimental results due to n → π* transition.

2.9 Practical application

To build the detection experiments operationally simple, user-friendly, and less expensive detection device for the on-site analysis of H_2S, cellulose paper Whatman 40 filter paper was used. It was immersed into the aqueous CH_3CN solution of **3-IA** (0.1 mg/mL) and then dried in air. The colourless white filter paper changed into yellow after spraying of an aqueous solution of Na_2S (Figure 8).

As it has shown, an obvious immediate colour change occurs under a UV hand lamp (Figure 8 bottom row), and an enhanced, rapid, and ratiometric colour change can be obtained from blue to green fluorescence in a longer time (3 min) that it could be clearly observed by the naked eye. These results exemplify the efficient application of **3-IA** for the advance of simple fluorimetric strips for H_2S detection.

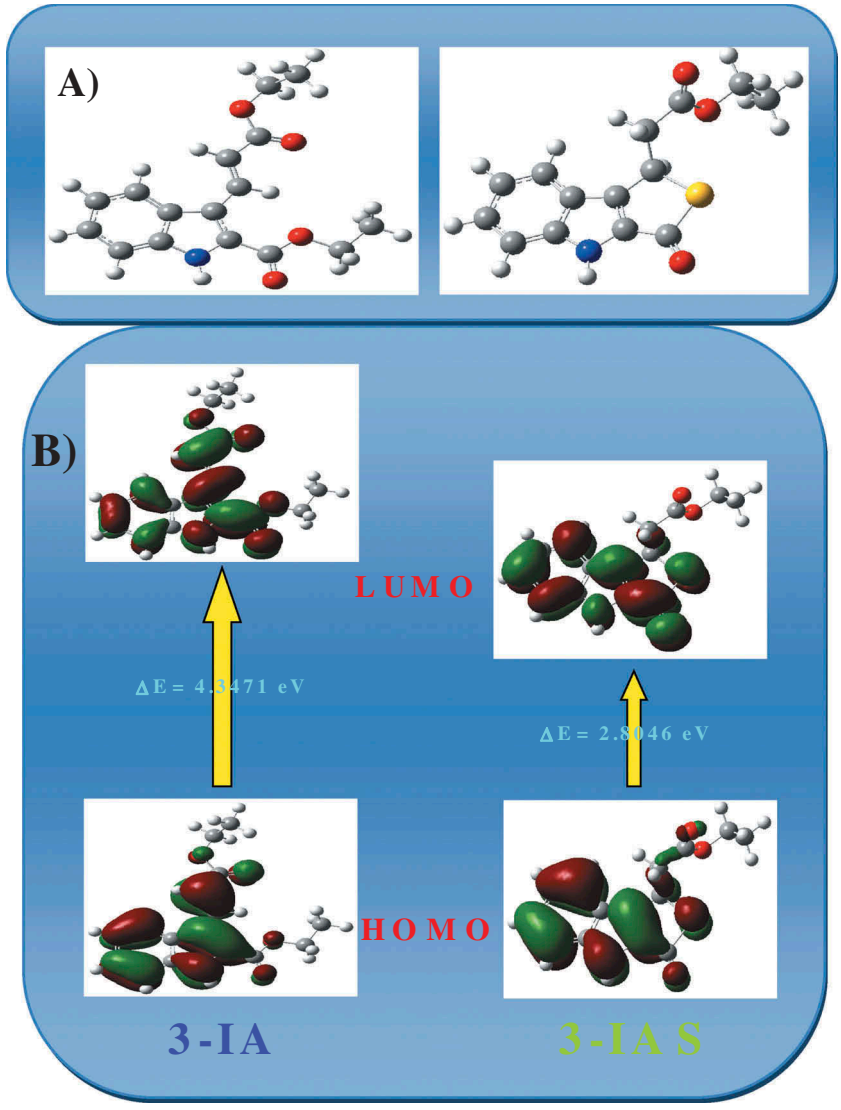

Figure 7. (colour online) (a) Energy-optimised structures of **3-IA** and **3-IAS**. (b) HOMO–LUMO distribution and energy difference of **3-IA** and **3-IAS.**

Now, we extend the application of our probe **3-IA** in detecting hydrogensulfide in presence of various industrial waste materials and different water sources. Though several interfering agents are present in natural surface water sources, yet we have successfully detected H_2S by using our probe **3-IA**. We collected various surface water samples from diverse parts of West Bengal, India (Supplementary Information, available online) and observed the potentiality of our probe **3-IA** in detecting H_2S in various surface water samples.

To carry out this experiment, we prepared 10 μM solutions of probe **3-IA** which were added to different water samples and emission spectral change observed upon addition of H_2S (12 equiv.). In case of all samples, significant fluorescence (at 463 nm) improvement was distinguished (Figure 9). No doubt these results showed that whatever is the source of water, enhancement in fluorescence of **3-IA** is revealed in the presence of H_2S only.

2.10 Cell imaging

Ideally, for cellular imaging experiments, higher excitation wavelengths are desirable. However, we were lucky enough to find that cells were able to survive our experiments with probe 3-IA which required excitation at 308 nm. Fluorescence imaging investigation was accomplished in Vero cells to reveal the practical applicability of the probe **3-IA** in biological systems. Prior to cell imaging, the MTT [3-(4,5-dimethyl-2-thiazolyl)-2,5-diphenyl-2- H-tetrazolium bromide] assay

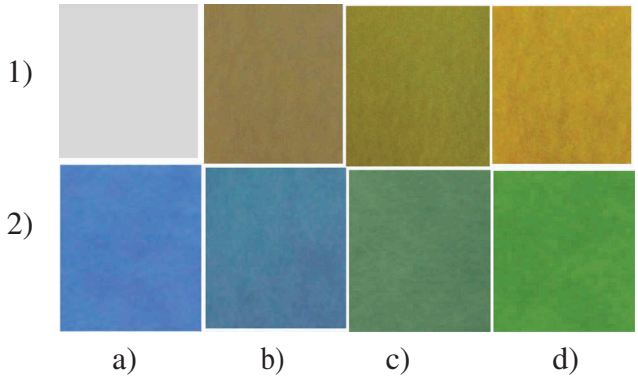

Figure 8. (colour online) (1) Naked eye colour changes visualised on TLC plate strips of (a) **3-IA** (c = 1.0×10^{-2}M) alone and after addition of H_2S at (b)1.0×10^{-4}M, (c) 1.0×10^{-3}M, and (d) 1.0×10^{-2}M in DMSO/H_2O = 1:9 (v/v). (2) Fluorescence colour changes visualised on TLC plate strips of (a) **3-IA** (c = 1.0×10^{-2}M) alone and after addition of H_2S at (b) 1.0×10^{-4}M, (c) 1.0×10^{-3}M, and (d) 1.0×10^{-2}M in DMSO/H_2O = 1:9 (v/v).

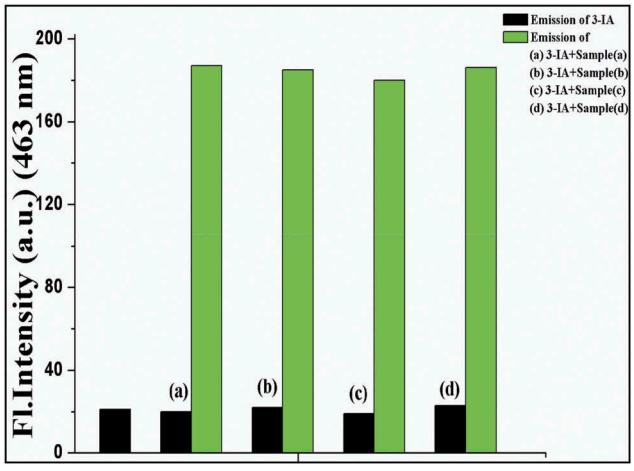

Figure 9. (colour online) Sensing of H_2S from surface water sample by using **3-IA.**

using the Vero cell line was carried out to evaluate the cytotoxicity of **3-IA**. As displayed in Figure S1 of the Supplementary Information, available online, it is observed that more than 80% of cells were viable even after 24 h incubation. The result stipulates little cytotoxicity of **3-IA**, while the concentration of **3-IA** was augmented up to 100 mg/mL.

To image the cells, a fluorescence microscope was used. Bright field images indicate that the cells were not injured in presence of the probe (Figure 10(a)) and H_2S (Figure 10(d)). When Vero cells were incubated with **3-IA** (1.0 μM) for 6 h, blue fluorescence was observed inside cells (Figure 10(b,c)). Upon addition of Na_2S (30.0 μM) to the above cells for another 8 h, a strong green emission inside cells was noticed (Figure 10(e,f)). This surveillance reveals that **3-IA** can detect the presence of H_2S in cells. Thus, the results indicate that **3-IA** is capable of detecting H_2S in living cells with satisfactory cell membrane permeability.

3. Synthesis and structure characterisation

3.1 Synthesis of 2

To a solution of indole-2-carboxylic acid (1) (1 g, 6.2 mmol) in 20 mL of ethanol, kept in an ice bath, four drops of sulfuric acid was added. Then, the reaction mixture was refluxed for 12 h with continuous TLC monitoring. After that, the mixture was cooled down to room temperature. After evaporation of the solvent in vacuum, the solid residue was purified by column chromatography on silica (eluted with 4% ethyl acetate/hexane) to afford the indole-2- ethyl carboxylate (2) (820 mg, 70%), a white solid.^{1}H-NMR ($CDCl_3$, 300 MHz): δ (ppm) 8.99 (s, 1H), 7.71 (d, 1H, J = 7.8 Hz), 7.44 (t, 1H, J = 6.9 Hz), 7.34 (m, 1H),7.26 (t, 1H,), 7.17 (m, 1H), 4.44 (q, 2H, J = 7.2 Hz), 1.44 (t, 3H, J = 7.2 Hz).

3.2 Synthesis of 3

In nitrogen atmosphere, 2 ml dry DMF was taken and then freshly distilled 2 ml phosphorus oxychloride ($POCl_3$) was added dropwise under ice-cold condition. The mixture was stirred until a red colouration arise. Then, indole-2-ethyl carboxylate (2) (500 mg, 2.65 mmol) dissolved in least amount of dry DMF was added to the previous mixture. Then, the whole mixture was heated to 50–60°C for 8 h. After completion of the reaction (evaluated by TLC monitoring), the mixture was cooled and poured into ice with stirring and then work up with ethyl acetate. The organic layer was dehydrated over sodium sulphate, and the solvents were evaporated under reduced pressure. The crude product was purified by column chromatography using (8% v/v) ethyl acetate-hexane to give pure aldehyde. White solid (200 mg, 35%). ^{1}H-NMR ($CDCl_3$, 300 MHz): δ (ppm) 10.67 (s, 1H), 8.34 (d, 1H, J = 8.1 Hz), 7.54 (d, 1H, J = 8.1 Hz), 7.32 (m, 2H),4.48 (q, 2H, J = 7.2 Hz), 3.06 (s, 1H), 1.46 (t, 3H, J = 7.2 Hz).

3.3 Synthesis of 3-IA

Compound 3 (100 mg, 0.46 mmol) was taken in dry ethanol. Then, diethyl malonate (110 mg, 0.69 mmol)

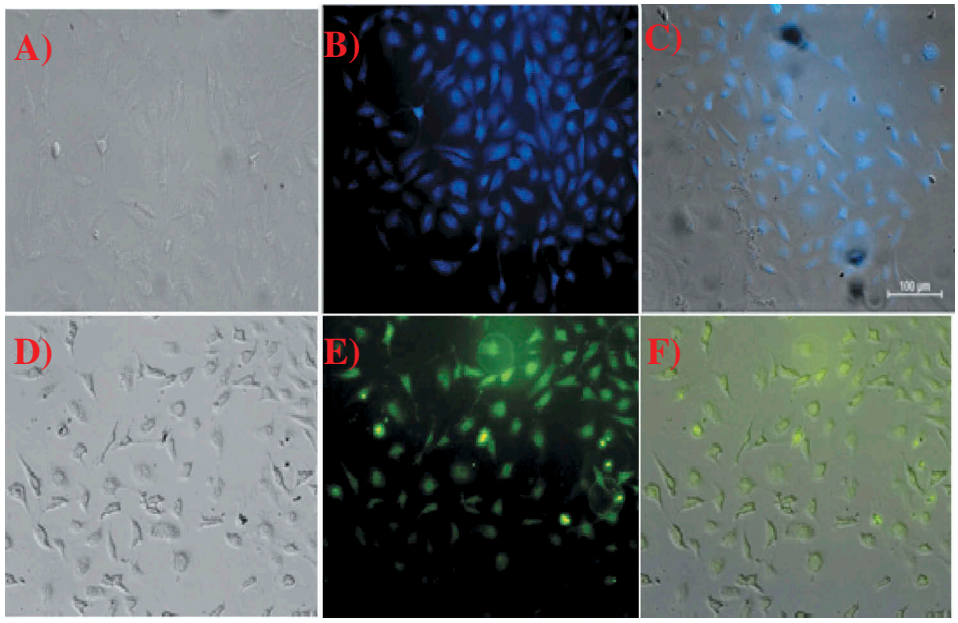

Figure 10. (colour online) Fluorescence images of probe in Vero cells (20× objective lens): (a) Bright field image of only cells treated with **3-IA** (1.0 μM). (b) Blue channel fluorescence images of cells treated with **3-IA** (1.0 μM) (blue channel, λ_{ex} = 308 nm, λ_{em} = 408 nm). (c) Merged image of **3-IA**. (d) Bright field image of **3-IA** (1.0 μM) treated with H_2S (30.0 μM). (e) Fluorescence image of **3-IA** (green channel, λ_{ex} = 308nm, λ_{em} = 463 nm) treated with 30.0 μMH_2S. (f) Merged image of **3-IA** treated with H_2S (30.0 μM) (scale bar: 100 μm).

and 0.5 ml piperidine were added and reflux for 24 h. In the end of the reaction (TLC monitoring), the solvent was removed under vacuum. Then, the solid product was purified by column chromatography over silica (eluted with 7% ethyl acetate/hexane) to afford the Light yellow solid (63 mg, 48%), mp:190–195°C, MS (LCMS): (m/z, %): 287.1 [100%]; calculated for $C_{16}H_{17}NO_4^+$: 287.06. ^{1}H-NMR (DMSO-d_6, 500 MHz): δ (ppm) 12.35 (s, 1H), 8.62 (d, 1H, J = 16.5 Hz), 8.0 (d, 1H, J = 8 Hz), 7.55 (d, 1H J = 3.5),7.37 (d, 1H, J = 7.7 Hz), 7.23 (t, 1H, J = 7.7),6.11 (d, 1H, J = 16.5 Hz), 4.41 (q, 2H, J = 7 Hz), 4.2 (q, 2H,J = 7 Hz), 1.35 (t, 3H, J = 7), 1.23 (t, 3H, J = 7 Hz). ^{13}C-NMR (DMSO-d_6, 100 MHz): 166.63, 160.71, 136.87, 127.18, 125.05, 121.76, 117, 115.39, 113.21, 61, 59.66, 39.59, 14.07.

3.4. Synthesis of the receptor 3-IA + H_2S adduct (3-IAS)

3-IA (50 mg, 0.17 mol) was taken in acetonitrile. Na_2S (70 mg, 0.85 mol) and few drops of water were added to it. The mixture was stirred about 30 min, and the resultant product was purified by column chromatography using 10% ethyl acetate in hexane (v/v) to give a white compound **3-IAS** (31 mg, 65%). Mp. 160–165°C. LCMS: (m/z, %): $[M]^+$calcd for $C_{14}H_{13}NO_3S$ is 275.06; Found: 275.1. ^{1}H-NMR ($CDCl_3$, 300 MHz): δ (ppm): 11.89 (s, 1H), 7.35(m, 4H), 4.31 (t, 1H, J = 7.2 Hz), 4.06 (q, 3H, J = 7.2 Hz), 3.29 (d, 2H, J = 7.2 Hz), 1.02 (t, 3H, J = 7.2 Hz).

4. Conclusion

In conclusion, we have planned and synthesised 3-indolylacrylate derivative, **3-IA**, by connecting an ethyl acrylate in 3-position. The probe itself showed blue emission, but upon reaction with H_2S, it ratiometrically turned into a compound which showed green emission. The probe **3-IA** is highly selective as well as sensitive towards H_2S and the sensing process is governed by intramolecular cyclisation reaction. X-ray data of the ratiometric probe showed that it has lateral intramolecular hydrogen bonding along with a pendant π…π stacking interactions. The formation of **3-IAS** has been recognised both experimentally and theoretically (DFT/TDDFT). Importantly, the ratiometric probe **3-IA** to be best employed for H_2S detection by simple visual fluorescent inspection in filter paper-based protocol. Additionally, furthermore, we have employed our probe to detect H_2S for ratiometric imaging in live Vero cell. Thus, this molecule not only demonstrates H_2S sensing efficiency but also brings to light a simple method of synthesising sulfur heterocycles fused with an indole moiety. The possibility of such a specific targeted chemical reaction can be explored in the design and

synthesis of the new fluorescent probe in the future for H_2S

Acknowledgements

We are grateful to DST-SERB [File No. EMR/2016/006640] for financial support. SSA and Dr AKP wish to acknowledge UGC-MANF (MANF-WES-67786) and SERB-NPDF, New Delhi, for the financial and research support.

Disclosure statement

No potential conflict of interest was reported by the authors.

Funding

We are grateful to DST-SERB [File No. EMR/2016/006640] for financial support. SSA and Dr AKP wish to acknowledge UGC-MANF (MANF-WES-67786) and SERB-NPDF, New Delhi, for the financial and research support.

References

(1) Kimura, H.; Nagai, Y.; Umemura, K.; Kimura, Y. *Antioxid.* **2005**, *7*, 795. doi: 10.1089/ars.2005.7.795
(2) He, J.; Huang, J.; He, Y.; Cao, P.; Zeller, M.; Hunter, A.D.; Xu, Z. *Chem. – Eur. J.* **2016**, *22*, 1597. DOI: 10.1002/chem.201504941.
(3) Bailey, T.S.; Pluth, M.D. *J. Am. Chem. Soc.* **2013**, *135*, 16697–16704. DOI: 10.1021/ja408909h.
(4) Yu, Q.; Gao, P.L.; Zhang, K.Y.; Tong, X.; Yang, H.R.; Liu, S. J.; Du, J.; Zhao, Q.; Huang, W.light: *Sci. Appl.* **2017**, *6*, e17107.
(5) Li, L.; Rose, P.; Moore, P.K. *Rev. Pharmacol. Toxicol*. **2011**, *51*, 169–187. DOI: 10.1146/annurev-pharmtox-010510-100505.
(6) Wang, R. *Physiol. Rev.* **2012**, *92*, 791–896. DOI: 10.1152/physrev.00017.2011.
(7) Fukuto, J.M.; Carrington, S.J.; Tantillo, D.J.; Harrison, J. G.; Ignarro, L.J.; Freeman, B.A.; Chen, A.; Wink, D.A. *Chem. Res. Toxicol.* **2012**, *25*, 769–793. DOI: 10.1021/tx2005234.
(8) Wu, P.; Zhang, J.; Wang, S.; Zhu, A.; Hou, X. *Chem. Eur. J.* **2014**, *20*, 952–956. DOI: 10.1002/chem.201303753.
(9) Liu, J.; Sun, Y.Q.; Zhang, J.; Yang, T.; Cao, J.; Zhang, L.; Guo, W. *Chem. Eur. J.* **2013**, *19*, 4717–4722. DOI: 10.1002/chem.201300455.
(10) Lin, V.S.; Lippert, A.R.; Chang, C.J. *Proc. Natl. Acad. Sci. U. S. A.* **2013**, *110*, 7131–7135. DOI: 10.1073/pnas.1302193110.
(11) Kimura., H. *Amino Acids*. **2011**, *41*, 113–121. DOI: 10.1007/s00726-010-0570-y.
(12) Singh, S.; Padovani, D.; Leslie, R.A.; Chiku, T.; Banerjee, R. *J. Biol. Chem.* **2009**, *284*, 22457. DOI: 10.1074/jbc.M109.010868.
(13) Reiffenstein, R.J.; Hulbert, W.C.; Roth, S.H. *Annu. Rev. Pharmacol. Toxicol.* **1992**, *32*, 109. DOI: 10.1146/annurev.pa.32.040192.000545.
(14) Shahrokhian, S. *Anal. Chem.* **2001**, *73*, 5972. DOI: 10.1021/ac010541m.
(15) Heafield, M.T.; Fearn, S.; Steventon, G.B.; Waring, R.H.; Williams, A.C.; Sturman, S.G. *Neurosci. Lett.* **1990**, *110*, 16. DOI: 10.1016/0304-3940(90)90814-P.
(16) Sachdev, P. *J. Neurol. Sci.* **2004**, *226*, 25. DOI: 10.1016/j.jns.2004.09.006.
(17) Giuliani, D.; Ottani, A.; Zaffe, D.; Galantucci, M.; Strinati, F.; Lodi, R.; Guarini, S. *Neurobiol. Learn. Mem.* **2013**, *104*, 82. DOI: 10.1016/j.nlm.2013.05.006.
(18) Cao, Q.; Zhang, L.; Yang, G.; Xu, C.; Wang, R. *Antioxid. Redox Signaling*. **2010**, *12*, 1101–1109. DOI: 10.1089/ars.2009.2915.
(19) Szabo, C. *Antioxid. Redox Signaling*. **2012**, *17*, 68–80. DOI: 10.1089/ars.2011.4451.
(20) Szabo, C.; Coletta, C.; Chao,; Modis, C.; Szczesny, K.B.; Pa-Papetropoulos, A.; Hellmich, M.R. *Natl. Acad. Sci. U. S. A.* **2013**, *110*, 12474–12479. DOI: 10.1073/pnas.1306241110.
(21) Liu, S.; Zhang, L.; Yang, T.; Yang, H.; Zhang, K.Y.; Zhao, X.; Lv, W.; Yu, Q.; Zhang, X.; Zhao, Q.; Liu, X.; Huang, W. *ACS Appl. Mater. Interfaces*. **2014**, *6*, 11013–11017. DOI: 10.1021/am5035158.
(22) Manibalan, K.; Mani, V.; Chang, P.C.; Huang, C.H.; Huang, S.T.; Marchlewicz, K.; Neethirajan, S. *Biosens. Bioelectron.* **2017**, *96*, 233–238. DOI: 10.1016/j.bios.2017.05.006.
(23) Ren, K.; Shang, X.; Chen, Y.; Zhang, X.; Fu, J.; Zhao, P.; Zhang, J. *Lumin*. **2017**, *32*, 765–771. DOI: 10.1002/bio.3248.
(24) Carter, K.P.; Young, A.M.; Palmer, A.E. *Chem. Rev.* **2014**, *114*, 4564. DOI: 10.1021/cr400546e.
(25) Zhu, H.; Fan, J.; Du, J.; Peng, X.A. *Chem. Res.* **2016**, *49*, 2115. DOI: 10.1021/acs.accounts.6b00292.
(26) Chen, X.; Pradhan, T.; Wang, F.; Kim, J.S.; Yoon, J. *Chem. Rev.* **2012**, 1910. DOI: 10.1021/cr200201z.
(27) Lin, V.S.; Chen, W.; Xian, M.; Chang, C.J. *Chem. Soc. Rev.* **2015**, *44*, 4596. DOI: 10.1039/C4CS00298A.
(28) Henthorn, H.A.; Pluth, M.D. *J. Am. Chem. Soc.* **2015**, *137*, 15330–15336. DOI: 10.1021/jacs.5b10675.
(29) Dai, C.G.; Liu, X.L.; Du, X.J.; Zhang, Y.; Song, Q.H. *ACS Sens.* **2016**, *1*, 888–895. DOI: 10.1021/acssensors.6b00291.
(30) Lippert, A.R.; New, E.J.; Chang, C.J. *J. Am. Chem. Soc.* **2011**, *133*, 10078–10080. DOI: 10.1021/ja203661j.
(31) Peng, H.; Cheng, Y.; Dai, C.; King, A.L.; Predmore, B. L.; Lefer, D.J.; Wang, B. *Angew. Chem. Int. Ed.* **2011**, *50*, 9672–9675. DOI: 10.1002/anie.201104236.
(32) Chen, B.; Li, W.; Lv, C.; Zhao, M.; Jin, H.; Jin, H.; Du, J.; Zhang, L.; Tang, X. *Analyst.* **2013**, *138*, 946–951. DOI: 10.1039/C2AN36113B.
(33) Yu, F.; Li, P.; Song, P.; Wang, B.; Zhao, J.; Han, K. *Chem. Commun.* **2012**, *48*, 2852–2854. DOI: 10.1039/c2cc17658k.
(34) Li, W.; Sun, W.; Yu, X. *J. Fluoresc*. **2013**, *23*, 181–186. DOI: 10.1007/s10895-012-1131-4.
(35) Zhang, L.; Zheng, X.E.; Zou, F.; Shang, Y.; Meng, W.; Lai, E.; Xu, Z.; Liu, Y.; Zhao, J. *Sci. Rep.* **2016**, *6*, 18868. DOI: 10.1038/srep18868.
(36) Montoya, L.A.; Pluth, M.D. *Chem. Commun.* **2012**, *48*, 4767–4769. DOI: 10.1039/c2cc30730h.
(37) Velusamy, N.; Binoy, A.; Bobba, K.N.; Nedungadi, D.; Mishra, N.; Bhuniya, S. *Chem. Commun.* **2017**, *53*, 8802–8805. DOI: 10.1039/C7CC05339H.

(38) Wu, M.Y.; Li, K.; Hou, J.T.; Huang, Z.; Yu, X.Q. *Org. Biomol. Chem.* **2010**, *10*, 8342–8347. DOI: 10.1039/c2ob26235e.
(39) Reja, S.I.; Kumar, N.; Sachdeva, R.; Bhalla, V.V.; Kumar, M. *RSC Adv.* **2013**, *3*, 17770–17774. DOI: 10.1039/c3ra42499e.
(40) Wang, R.; Yu, F.; Chen, L.; Chen, H.; Wanga, L.; Zhanga, W. *Chem. Commun.* **2012**, *48*, 11757–11759. DOI: 10.1039/c2cc36088h.
(41) Nickson, T.E. *J. Org. Chem.* **1986**, *51*, 3903–3904. DOI: 10.1021/jo00370a031.
(42) Wu, Z.; Liang, D.; Tang, X. *Anal. Chem.* **2016**, *88*, 9213–9218. DOI: 10.1021/acs.analchem.6b02459.
(43) Pak, Y.L.; Li, J.; Ko, K.C.; Kim, G.; Lee, J.Y.; Yoon, J. *Anal. Chem.* **2016**, *88*, 5476–5481. DOI: 10.1021/acs.analchem.6b00956.
(44) Chen, Y.; Zhu, C.; Yang, Z.; Chen, J.; He, Y.; Jiao, Y.; He, W.; Qiu, L.; Cen, J.; Guo, Z. *Angew. Chem. Int. Ed.* **2013**, *52*, 1688. DOI: 10.1002/anie.201207701.
(45) Paul, S.; Goswami, S.; Mukhopadhyay, C.D. *New J. Chem.* **2015**, *39*, 8940. DOI: 10.1039/C5NJ01297J.
(46) Feng, X.; Zhang, T.; Liu, J.-T.; Miao, J.-Y.; Zhao, B.-X. *Chem. Commun.* **2016**, *52*, 3131. DOI: 10.1039/C5CC09267A.
(47) Guria, U. N.; Maiti, K.; Ali, S. S.; Samanta, S. K.; Mandal, D.; Sarkar, R.; Datta, P.; Ghosh, A. K.; Mahapatra, A. K. *New J. Chem.* **2018**, *42*, 5367–5375. DOI: 10.1039/C7NJ04632D.
(48) Pritchard, R.B.; Lough, C.E.; Currie, D.J.; Holmes,; Can., H. L. *J. Chem.* **1968**, *46*, 775–781. doi: 10.1139/v68-128
(49) Liu, C.; Peng, B.; Li, S.; Park, C.M.; Whorton, A.R.; Xian, M. *Org. Lett.* **2012**, *14*, 2184. DOI: 10.1021/ol3008183.
(50) Liu, C.; Pan, J.; Li, S.; Zhao, Y.; Wu, L.Y.; Berkman, C.E.; Whorton, A.R.; Xian, M. *Angew. Chem. Int. Ed.* **2011**, *50*, 10327. DOI: 10.1002/anie.201104305.
(51) Peng, B.; Chen, W.; Liu, C.; Rosser, E.W.; Pacheco, A.; Zhao, Y.; Aguilar, H.C.; Xian, M. *Chem. Eur. J.* **2014**, *20*, 1010. DOI: 10.1002/chem.201303757.
(52) Xu, Z.; Xu, L.; Zhou, J.; Xu, Y.; Zhu, W.; Qian, X. *Chem. Commun.* **2012**, *48*, 10871. DOI: 10.1039/c2cc36141h.
(53) Choi, M.G.; Cha, S.; Lee, H.; Jeon, H.L.; Chang, S.-K. *Chem. Commun.* **2009**, 7390. DOI: 10.1039/b916476f.
(54) Sasakura, K.; Hanaoka, K.; Shibuya, N.; Mikami, Y.; Kimura, Y.; Komatsu, T.; Ueno, T.; Terai, T.; Kimura, H.; Nagano, T. *J. Am. Chem. Soc.* **2011**, *133*, 18003. DOI: 10.1021/ja207851s.
(55) Hou, F.; Huang, L.; Xi, P.; Cheng, J.; Zhao, X.; Xie, G.; Shi, Y.; Cheng, F.; Yao, X.; Bai, D.; Zeng, Z. *Inorg. Chem.* **2012**, *51*, 2454. DOI: 10.1021/ic2024082.
(56) Hou, F.; Cheng, J.; Xi, P.; Chen, F.; Huang, L.; Xie, G.; Shi, Y.; Liu, H.; Bai, D.; Zeng, Z. *Dalton Trans.* **2012**, *41*, 5799. DOI: 10.1039/c1dt11660f.
(57) Santos-Figueroa, L.E.; de la Torre, C.S.; Sayed, E.; Sanceno, F.; Martı´nez-Ma´n˜ez, R.; Costero, A.M.; Gil, S.; Parra, M. *Eur. J. Inorg. Chem.* **2014**, *41*. doi: 10.1002/ejic.201301306
(58) Velusamya, N.; Thirumalaivasan, N.; Bobba, K.,.N.; Wu, S.,.P.; Bhuniya, S. *New J. Chem.* **2018**, *42*, 1590–1594. DOI: 10.1039/C7NJ04119E.
(59) Li, X.; Zhang, S.; Cao, J.; Xie, N.; Liu, T.; Yang, B.; He, Q.; Hu, Y. *Chem. Comm.* **2013**, *49*, 8656–8658. DOI: 10.1039/c3cc44539a.